

9th International Conference on Photonic Technologies - LANE 2016

Effect of powder size and shape on the SLS processability and mechanical properties of a TPU elastomer

Sasan Dadbakhsh^{a,*}, Leander Verbelen^b, Tom Vandeputte^a, Dieter Strobbe^a,
Peter Van Puyvelde^b, Jean-Pierre Kruth^a

^aPMA, Department of Mechanical Engineering, KU Leuven, Leuven, Belgium

^bDepartment of Chemical Engineering, KU Leuven, Leuven, Belgium

Abstract

This work investigates the influence of powder size/shape on selective laser sintering (SLS) of a thermoplastic polyurethane (TPU) elastomer. It examines a TPU powder which had been cryogenically milled in two different sizes; coarse powder ($D_{50} \sim 200 \mu\text{m}$) with rough surfaces in comparison with a fine powder ($D_{50} \sim 63 \mu\text{m}$) with extremely fine flow additives. It is found that the coarse powder coalesces at lower temperatures and excessively smokes during the SLS processing. In comparison, the fine powder with flow additives is better processable at significantly higher powder bed temperatures, allowing a lower optimum laser energy input which minimizes smoking and degradation of the polymer. In terms of mechanical properties, good coalescence of both powders lead to parts with acceptable shear-punch strengths compared to injection molded parts. However, porosity and degradation from the optimum SLS parameters of the coarse powder drastically reduce the tensile properties to about one-third of the parts made from the fine powders as well as those made by injection molding (IM).

© 2016 Published by Elsevier B.V. This is an open access article under the CC BY-NC-ND license

(<http://creativecommons.org/licenses/by-nc-nd/4.0/>).

Peer-review under responsibility of the Bayerisches Laserzentrum GmbH

Keywords: Selective laser sintering (SLS); Processability; Powder morphology; Thermoplastic polyurethane (TPU) polymer

1. Introduction

Selective laser sintering (SLS) is one of the main polymer additive manufacturing (AM) techniques, in which three-dimensional parts are constructed by fusing polymer powders in a layer-by-layer approach. Consolidation in each layer is performed by laser sintering of selected regions on top of the powder heated to a specific temperature.

* Corresponding author. Tel.: +32-163-72866 ; fax: +32-163-22987 .

E-mail address: sasan.dadbakhsh@kuleuven.be

Accordingly, this process is affected by a multitude of factors from powder composition and morphology to laser energy input and processing (or powder bed) temperature.

Among thousands of polymeric materials, there are only few grades of polymers that are commercially available for the SLS process. The vast majority of these SLS polymers belong to thermoplastic materials due to their viscous coalescence at higher temperatures. This includes amorphous, semicrystalline, reinforced and filled polymers. Among SLS polymers, semicrystalline polyamide (mainly PA12 (Hadi et al. 2009)) is dominant, however, new research is exploring other semicrystalline and amorphous families such as polyetheretherketone (PEEK) (Ghita et al. 2014), polystyrene (PS) (Wang et al. 2011), polypropylene (Zhu et al. 2015), thermoplastic elastomers (Ziegelmeier et al. 2015), etc. The common difficulties with these new polymers include porosity, poor coalescence, warpage, low flowability, degradation and recyclability (Kruth et al. 2007, Goodridge et al. 2012, Bourell et al. 2014, Schmid et al. 2014).

As many SLS processing issues originate from the used powder, many research works are now dedicated to characterize the original powders and link the results to the SLS processability (Ziegelmeier et al. 2013, Wudy et al. 2014, Ziegelmeier et al. 2015, Verbelen et al. 2016). For example, Verbelen et al. (Verbelen et al. 2015, Verbelen et al. 2016) have studied the morphology, melt flow, coalescence and melting/crystallization of some commercial PA12, PA11, and PA6 powders to give a practical demonstration on the powder SLS processability. Furthermore, Wudy et al. (Wudy et al. 2014) have investigated the surface tension of a commercial PA12 powder melt to explain powder coalescence in SLS. Other studies have mainly focused on actual SLS behavior of the powders via visual process progress, porosity content, warpage, and mechanical properties of the products (Kruth et al. 2007, Goodridge et al. 2012, Bourell et al. 2014). All these examinations are essential to generate a comprehensive knowledge to develop new SLS polymers, including elastomer families (which their high flexibility is extremely attractive for different applications).

Despite some previous works of Ziegelmeier et al. on powder flow and SLS properties of few grades of thermoplastic polyurethane (TPU) elastomers (Ziegelmeier et al. 2013, Ziegelmeier et al. 2014, Ziegelmeier et al. 2015), the effect of the morphology of the powder is still poorly understood. Accordingly, this work systematically analyses two different morphologies of the same TPU grade when they are exposed to the SLS process. In this respect, morphologies, packing densities, thermal behaviors and coalescences of these powders are investigated. The results are linked to the processability at various temperatures, outcome density, and tensile and shear punch strength of the SLS products and are compared to injection molding (IM) parts. This provides necessary knowledge for developing new grades of TPU elastomers by powder and additive manufacturers.

2. Materials and experiments

2.1. Materials and powder characterizations

In this work, a TPU powder grade (new to the SLS process) was investigated. The provided TPU possessed a density of 1.21 g/cm^3 , a shore A hardness of $\sim 85\text{-}89 \text{ A}$, and a gradual softening behavior upon heating (see DSC in section 3.1). The supplied TPU powders were cryogenically milled in two different sizes (Fig. 1); coarser powders with coarse edges (Fig. 1a) in comparison with finer powders with relatively smoother edges (the fine powder is covered by some small additives improving the powder flowability, Fig. 1b). The particle size distribution (PSD) was measured using a Malvern Mastersizer micro plus that uses laser diffraction to determine the particle sizes of the TPU powders suspended in ethanol. The packing density was also determined in a Copley JV 1000, as the proportion of the tapped powder mass to its volume (measured in a 100 ml graduated cylinder). This was normalized by dividing by the polymer material density.

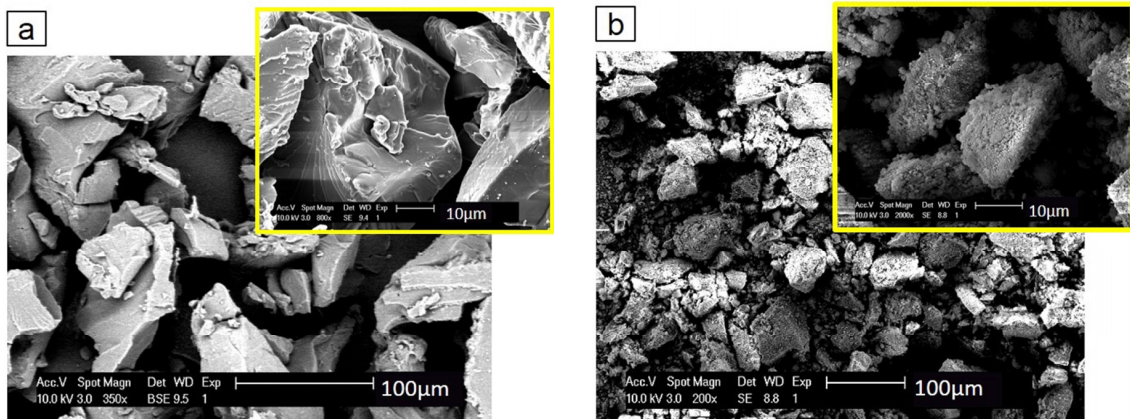


Fig. 1. (a) Coarse and (b) fine powders from a TPU grade.

Differential scanning calorimetry (DSC) was carried out using a TA instruments DSC Q2000 (under a nitrogen inert atmosphere) to derive the thermal properties of the powders. Heating and cooling cycles were performed between -70°C and 200°C with a rate of $10^{\circ}\text{C}/\text{min}$. The coalescence behavior of the powders was also directly visualized on a hot stage microscope (Olympus BX41), using a shear cell for heating (Linkam CSS450) with 10x magnification and heating rate of $10^{\circ}\text{C}/\text{min}$.

2.2. Selective laser sintering (SLS) processing

SLS was performed on a DTM Sinterstation 2000, equipped with a CO_2 laser (wavelength $\sim 10.6\ \mu\text{m}$) with Gaussian power distribution and a full diameter of $400\ \mu\text{m}$. The N_2 -atmosphere is set at an upper limit of 5.5% oxygen. Single layer tests were first performed at different temperatures to assess a preliminary understanding of SLS processability before manufacturing multilayer parts. For these tests, the laser power was varied between 3 W and 27 W at a constant scanning speed of 1000 mm/s and scan spacing of $150\ \mu\text{m}$. For multilayer parts, the layer thickness was $100\ \mu\text{m}$. The processing temperatures were individually optimized and selected for the coarse and fine powders (as will be presented in the results and discussion section). The energy density (E) was calculated according to the Equation 1 (see below), combining laser power (P), scan speed (v) and scan spacing (s). As the part layout, the laser scan tracks were oriented in the longitudinal direction of the samples and tensile bars.

$$E = \frac{P}{s \cdot v} \quad (\text{J}/\text{mm}^2) \quad (1)$$

2.3. Injection molding (IM) references

Injection molding (IM) was used to manufacture reference parts from the coarse TPU powder (the IM parts are considered as fully dense). IM heats the powder in a small chamber at 170°C (where it is molten). A plunger then pushes the molten plastic from the chamber into a tensile bar die at room temperature, where it cools and consolidates. No significant sign of degradation (such as smoke or discoloration) was visually observed during IM.

2.4. Part characterizations

Densities of the manufactured components ($\sim 51\ \text{mm} \times 21\ \text{mm} \times 4\ \text{mm}$) were determined by both dimensional and Archimedes methods (according to at least two measured parts). With the dimensional method, the density is calculated by dividing the weight of a cuboid part by its metered volume. ‘Archimedes’ densities were also calculated from the weight measurements in air and in demineralized water. Since Archimedes measurements may

carry some uncertainty in presence of open porosity (due to fluid penetration into the open pores), this method was only performed on relatively dense parts or the parts with no surface connected porosity (such as the IM parts or the SLS samples with lower porosity).

Tensile tests were carried out on the IM parts as well as the SLS samples (made using the parameters reaching maximum densities). At least three samples in a 'dogbone' shape (Fig. 2a) were stretched for each tensile measurement using an Instron 5567 with a 1 kN load cell and 1 kN pneumatic clamps at room temperature. A crosshead speed of 50 mm/min was maintained till sample failure. Since elastomers typically show a very large elongation, the strain was calculated as the ratio of the extension of the clamps to the initial distance between the two clamps. Engineering stress and strains were reported.

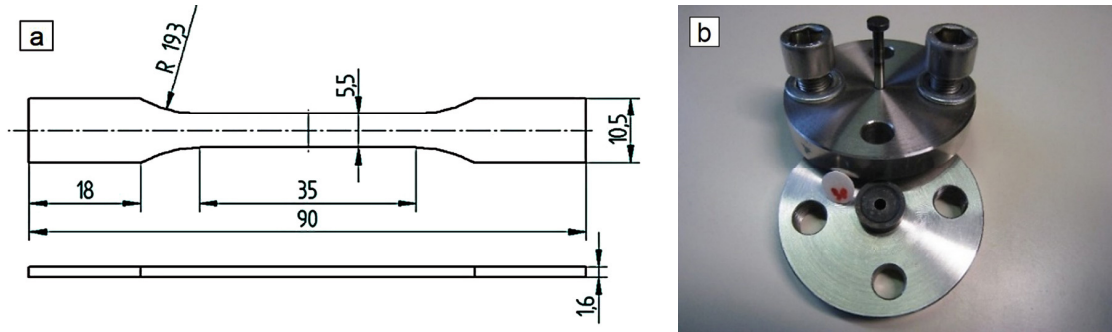


Fig. 2. (a) Schematic demonstration of tensile bars and (b) shear-punch apparatus used in this work.

Shear punch testing (SPT) was used as a demonstration for the shear strength and adhesion quality between the sintered powder layers (Rider 1977). The SPT measurements were performed on an Instron 5567 with a compression set-up and a load cell of 1 kN. Fig. 2b shows the hardened steel shear punch tool, with an SLS sample. The pin or punch ($D_{\text{punch}} = 5.0\text{mm}$) pushes the material through the die hole ($D_{\text{die}} = 5.2\text{mm}$), thereby loading it with shear stress. The compression rate was fixed at 1mm/min. The sample thickness (t) which was about 1.0-1.5 mm in this work. The shear stress (as the primary outcome of the test) is calculated as (Guduru et al. 2005):

$$\tau = \frac{F}{2\pi r_{\text{avg}} t \rho_r} \quad (2)$$

where $r_{\text{avg}} = \frac{r_{\text{punch}} + r_{\text{die}}}{2}$, F is the applied load and t is the specimen thickness. ρ_r is the relative density (equal to 1 for a 100% dense part) and added to compensate the lowered shearing surface due to presence of porosity. The sample thickness (t) which was about 1.0-1.5 mm in this work.

3. Results and discussion

3.1. Powder characteristics

Fig. 3 shows the particle size distribution and packing density of the TPU powders tested in this work. As seen for the fine powder, the smaller average particle size of about 63 μm (between 6-140 μm containing flow additives) has led to a normalized packing density of about 40.6%. This is about 50% more than the normalized packing density of the coarser powder (~26.6%) with an average particle size of 200 μm . The improved packing density may result in a better layer packing during the SLS process and increase the quality/density of the products.

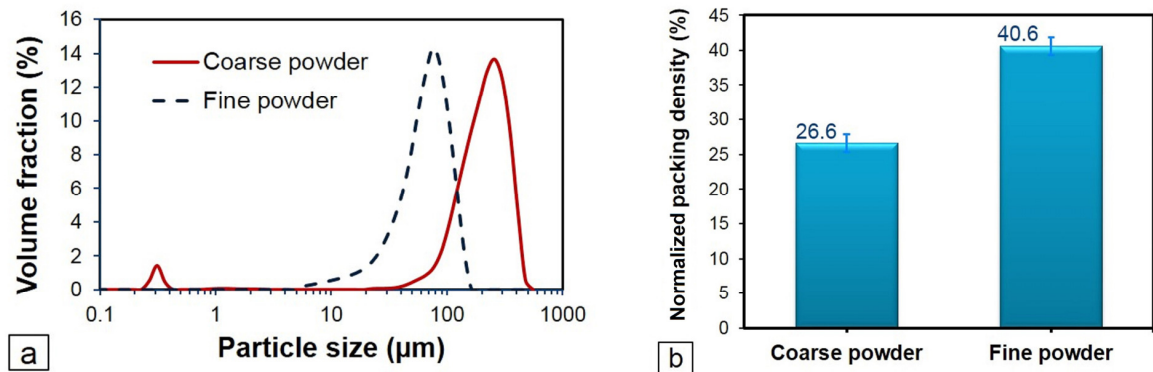


Fig. 3. (a) Particle size distribution (PSD) and (b) packing density of coarse and fine powders used in this work.

To select a proper preheating/powder bed temperature for the SLS processing, the thermal properties of the TPU powders were first determined using DSC tests (Fig. 4). The measured thermal properties are direct outcome of polymer constituents, being composed of hard and soft segments in TPUs. As seen, both fine and coarse powders show similar thermal behavior; they show some crystallization during the cooling down stage from 200°C (around 71°C, probably due to crystallization of hard segments). Glass transition of these TPUs are far below normal operating temperatures (due to soft segments), giving them elastomeric properties. This glass temperature, however, plays no significant role in SLS parameter selection (as TPU is perfectly solid at higher temperatures before softening of hard segments occurs). In fact, it is the hard segments that melt via heating in a broad temperature range, providing the necessary viscous flow for a successful SLS process.

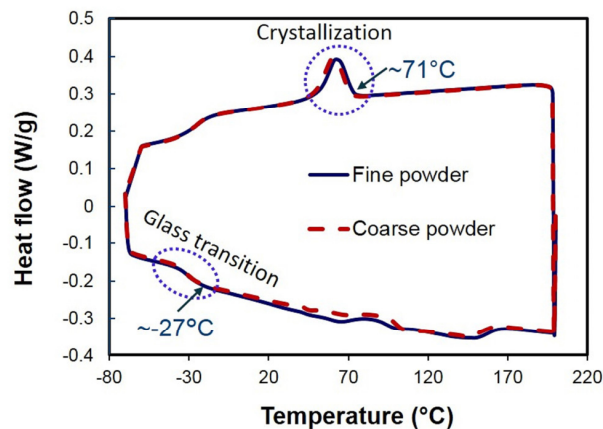


Fig. 4. Differential scanning calorimetry (DSC) curves showing similar transitions for fine and coarse TPUs.

Apart from DSC, hot stage microscopy was also performed to compare the coalescence behavior of the powders (as shown in Fig. 5). The results, despite the DSC behavior, is evidently distinguished between the coarse and fine powders. In fact, the coarser powder coalesces faster at lower temperatures (Fig. 5a) in contrast to fine powder that is still highly viscous at 150°C (Fig. 5c). At 180°C, where the coarse powder is now highly fluid (Fig. 5b), the fine powder just starts to reach a low viscosity (Fig. 5d) which is essential for SLS. This behavior is perhaps due to presence of very small additives (such as hydrated silicas, glassy oxides, fluoroplastics and metallic stearates), primarily added to facilitate the powder flow and improve the packing efficiency (Goodridge et al. 2012). These

small additives decorate the fine powder surfaces (see Fig. 1) that may delay the viscous flow temperature of the fine TPU powder, but they will not affect the DSC results within the experimented temperature range (see Fig. 4).

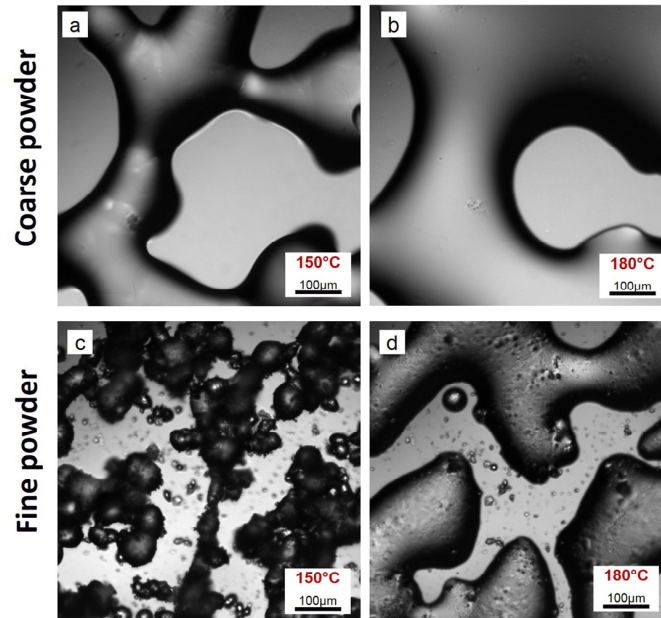


Fig. 5. Powder coalescence (observed by hot stage microscopy during heating with a constant heating rate) of a-b) coarse and c-d) fine powders at 150°C and 180°C.

3.2. SLS processability and density optimizations (from single layer to multilayer parts)

After studying the primary powder characteristics, SLS experiments were performed to manufacture TPU parts. At first, single layer tests were carried out as a shortcut to get a first impression of the powder sinterability in a wide range of laser energy input. These experiments on the coarse powder, as shown in Fig. 6a, demonstrate a minimum required sinterability; the part can be made but the poor packing and poor powder flow lead to a ribbed-like pattern on sintered parts. Although higher processing temperatures (i.e., over 75°C) could potentially improve the sintering quality, this was not possible due to excessive powder caking that appears at those temperatures. In contrast to coarse powders, finer powder flowed better leading to a good packing during the SLS process (Fig. 6b). Moreover, a higher powder bed temperature ($\sim 105^{\circ}\text{C}$) was possible due to the presence of flow additives (restricting caking at this processing temperature). The combination of better flow and higher processing temperature led to good sintered parts with smooth appearances (as seen in Fig. 6b). It should also be noted that smoking occurred in both cases (being excessive especially at high laser energy input). This smoking is a sign of degradation that can potentially damage the product properties.

After evaluating the processing temperature for these powders in single layer experiments, multilayer parts were manufactured to find the maximum reachable densities. As shown in Fig. 7, the optimum energy input is much lower for the fine powder compared to that required for the coarse one; for the fine powder the optimum energy is about 0.067 J/mm^2 while it is about 0.160 J/mm^2 for the coarse powder. The lower energy input is enabled by a higher bed temperature that was utilized for the fine powder (a higher bed temperature requires less laser energy to melt the powder (Tontowi et al. 2001, Bourell et al. 2014)). The higher bed temperature correlates with the higher flowability of the finer powder and improves the density of products ($\sim 95\%$ in comparison with $\sim 87\%$ relative density of the parts from the coarse powder).

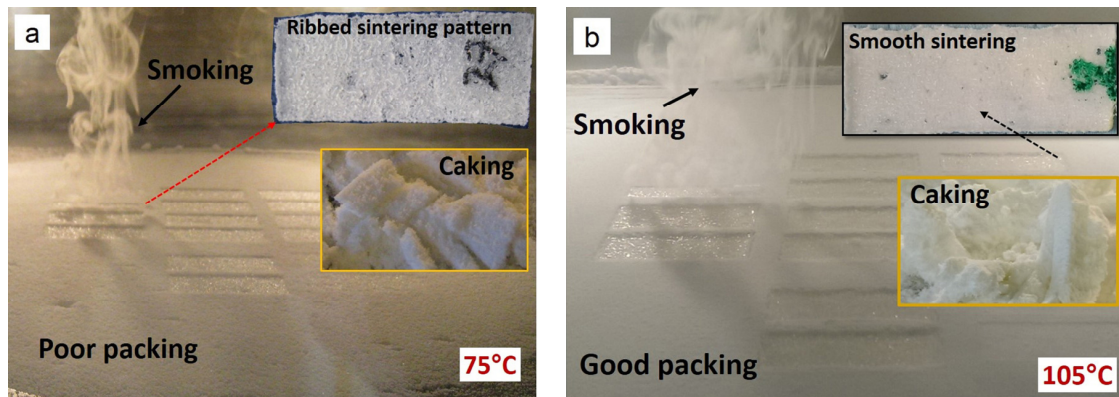


Fig. 6. Visual SLS specifications of (a) coarse and (b) fine TPU powders.

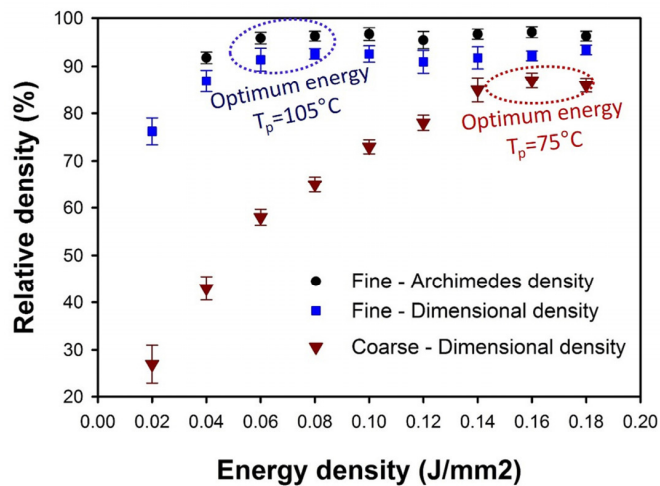


Fig. 7. Relative density of the SLS parts made from coarse and fine TPU powders as a function of the input laser energy density. Note that processing temperature (T_p) was 75°C and 105°C for coarse and fine powders, respectively.

3.3. Heat of crystallization after SLS

As previously shown (Fig. 4), the current TPU powders exhibit a crystallization peak during cooling down from 200°C. This crystallization peak is also present for the IM and SLS manufactured parts (Fig. 8a). Since all these parts go through a full remelting at 200°C, it can be assumed that a higher enthalpy of crystallization corresponds to more hard segments that are available for crystallization. The alterations in the number of these hard segments can be attributed to the influence of laser energy input that degrades and annihilates the polymer structures. This is better shown in Fig. 8b, where the enthalpy of crystallization of the IM part (~97% of the original powder) is near the SLS part made from the fine powder (~96% of the original powder). The enthalpy of crystallization, however, drops to 70% for the SLS part made from coarse powder ($E = 0.160 \text{ J/mm}^2$). This is particularly important since the lower enthalpy of crystallization corresponds to lower number of hard segments (lowered by degradation). This may reduce the mechanical properties, as the hard segments have the main contribution to strength of TPUs.

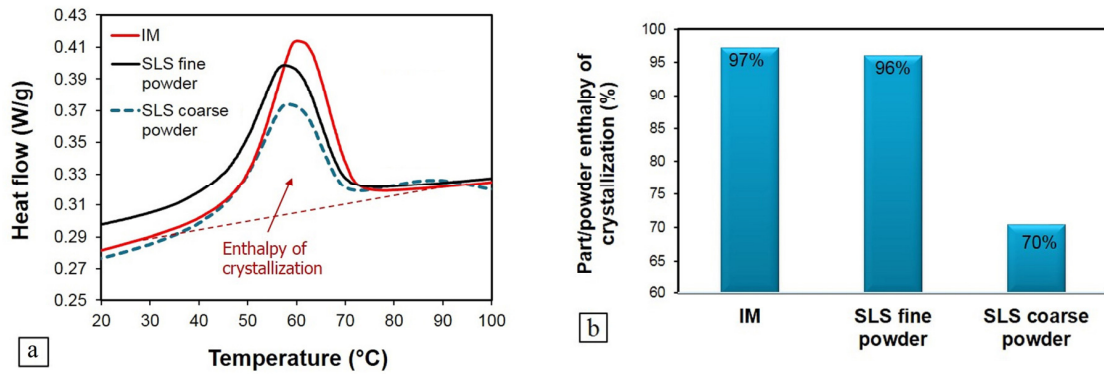


Fig. 8. DSC enthalpy of crystallization occurring via cooling from 200°C; a) DSC curves showing the heat flow around crystallization temperature and b) relative enthalpy of IM and SLS parts to powder. The SLS parts are from the fine powder (made by $E = 0.067 \text{ J/mm}^2$) and the coarse powder (made by $E = 0.160 \text{ J/mm}^2$).

3.4. Mechanical properties

After optimizing the processing parameters, tensile bars were manufactured to explore the mechanical properties of the products (as shown in Fig. 9). As seen, the coarse powder leads to SLS parts with the lowest tensile properties, compared to finer powders that can reach tensile properties close to those of IM parts. This large difference in tensile properties can be attributed to the SLS processing conditions. In fact, the lower energy input of 0.067 J/mm^2 at higher powder bed temperature of 105°C allows 95% dense parts with minimum degradation (minimal smoking was visually observable) from the fine powder. This leads to tensile strengths ($\sim 17.8 \pm 1.5 \text{ MPa}$) and elongations ($\sim 559 \pm 33\%$) which are comparable to those from IM parts. In contrast, the lower processing temperature ($\sim 75^\circ\text{C}$) and the higher energy input ($\sim 0.160 \text{ J/mm}^2$) for coarser powder lead to more porosity ($\sim 87\%$) and smoking (corresponding to degradation of hard segments that have a main contribution to part strength), drastically reducing the UTS (26% of IM) and elongation (37% of IM).

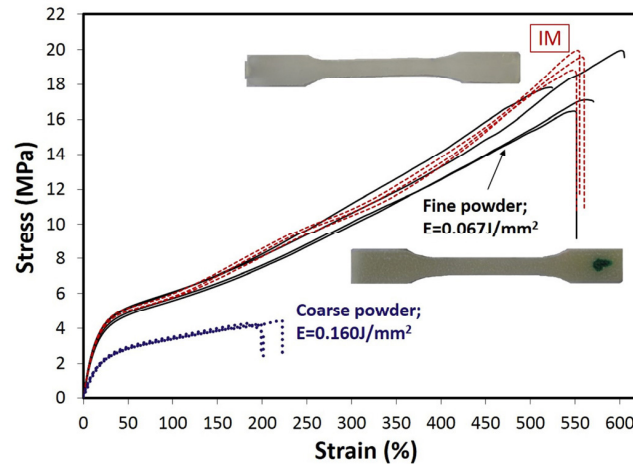


Fig. 9. Tensile behaviors of the optimum SLS parts (from the fine and coarse powders) in comparison with the IM parts. Each test has been repeated at least 3 times as shown in tensile curves.

In addition to tension, shear-punch tests were performed as a demonstration for adhesion quality and sintering performance of the powders. The result is shown in Table 1 (along with the summary of density and tensile properties for comparison). As seen, the shear strength of the SLS parts from the fine powders is also comparable to the shear strength of IM parts. In fact, higher powder bed temperature has compensated the lower SLS energy input ($E=0.067 \text{ J/mm}^2$) and provided comparable IM sintering. In contrast, SLS parts from the coarse powder show somehow lower shear strengths (i.e. 84% of IM), associated with a lower bonding/coalescence degree due to lower processing temperatures. Since the shear strength has not been altered as much as tensile properties by the energy input, one may perhaps postulate that soft segments have been the main responsible for bonding, but they are not affected as much by degradation. Nevertheless, Table 1 exhibits the fine powder as a potential material for SLS of quality TPU elastomers with a performance near to IM parts.

Table 1. Overview of used parameters, density, tensile properties and shear-punch strengths of the optimum SLS parts (made from coarse and fine powders) in respect to the properties of IM parts. Notice that porosity of optimum SLS parts has been compensated in shear stress calculations (equation 2).

Condition	SLS temperature (°C)	SLS energy (J/mm ²)	Relative density	UTS (MPa)	UTS vs IM	Elongation at break (%)	Elongation vs IM	Shear strength	Shear strength vs IM
IM	N/A	N/A	100%	19.4±0.5	100%	556	100%	9.9	100%
SLS-Fine	105	0.067	95±2.5%	17.8±1.5	92%	559±33	100%	9.8±1.7	99.90%
SLS-Coarse	75	0.160	87±2.5%	4.3±0.1	26%	208±13	37%	8.3±0.5	84%

4. Summary

This work analyzed the SLS processability of one TPU grade but provided in two different powder forms: i) fine powder with submicron and nano-size flow additives and ii) coarse powders without any flow additive particles. It was shown that despite the same DSC behavior of both powders, the finer powders allowed a much higher processing temperature ($\sim 105^\circ\text{C}$ vs. $\sim 75^\circ\text{C}$ for the coarse powder) associated with the presence of flow additives. As the processing temperature was higher for the fine powder, maximum density was achieved at a significantly lower energy density. Furthermore, higher flow and better packing of the fine powder contributed to a higher obtainable density of the SLS parts.

Smoking was also another important phenomenon that abundantly occurred at higher SLS energies. The lower optimum SLS energies for the finer powder, however, allowed a minimal smoking as a sign of degradation of TPU segments. The lower degradation was reflected in the enthalpy of crystallization (from hard TPU segments) as well as the mechanical properties; optimum SLS part from the fine powder showed a high crystallization enthalpy ($\sim 96\%$ of the TPU powder) as well as a tensile strength and elongation comparable to those from IM. This was different from the coarse powder that led to SLS parts with $\sim 70\%$ powder crystallization enthalpy as well as a UTS and elongation around 26% and 37% of the IM parts, respectively. Furthermore, the higher processing temperature of the fine powder provided a better coalescence quality, as confirmed by the resulting IM comparable shear-strengths. In summary, the fine TPU powder with flow additives allowed for higher processing temperature, higher part density, and lower required SLS energy which led to high-quality SLS parts (even in comparison with IM). These findings highlighted the importance of the powder morphology for the SLS process.

Acknowledgements

The authors acknowledge the Flemish support from Strategic Initiative Materials in Flanders (SIM) and the agency for Innovation by Science and Technology (IWT) within the framework of SIM-SBO-STREAM project PolyForce.

References

- Bourell, D.L., Watt, T.J., Leigh, D.K., Fulcher, B., 2014. Performance Limitations in Polymer Laser Sintering. *Physics Procedia* 56, 147-156.
- Ghita, O.R., James, E., Trimble, R., Evans, K.E., 2014. Physico-chemical behaviour of Poly (Ether Ketone) (PEK) in High Temperature Laser Sintering (HT-LS). *Journal of Materials Processing Technology* 214, 969-978.
- Goodridge, R.D., Tuck, C.J., Hague, R.J.M., 2012. Laser sintering of polyamides and other polymers. *Progress in Materials Science* 57, 229-267.
- Guduru, R.K., Darling, K.A., Kishore, R., Scattergood, R.O., Koch, C.C., Murty, K.L., 2005. Evaluation of mechanical properties using shear-punch testing. *Materials Science and Engineering: A* 395, 307-314.
- Hadi, Z., Candice, M., Neil, H., 2009. Degree of particle melt in Nylon-12 selective laser-sintered parts. *Rapid Prototyping Journal* 15, 126-132.
- Kruth, J.-P., Levy, G., Klocke, F., Childs, T.H.C., 2007. Consolidation phenomena in laser and powder-bed based layered manufacturing. *CIRP Annals - Manufacturing Technology* 56, 730-759.
- Rider, M., 1977. The shear strength of enamel — composite bonds. *Journal of Dentistry* 5, 237-244.
- Schmid, M., Amado, A., Wegener, K., 2014. Materials perspective of polymers for additive manufacturing with selective laser sintering. *Journal of Materials Research* 29, 1824-1832.
- Tontowi, A.E., Childs, T.H.C., 2001. Density prediction of crystalline polymer sintered parts at various powder bed temperatures. *Rapid Prototyping Journal* 7, 180-184.
- Verbelen, L., Dadbakhsh, S., Kruth, J.-P., Van Puyvelde, P., 2015. Characterization of different PA powders to determine their applicability for laser sintering. *Solid Freeform Fabrication Symposium (SFF)*, Austin, Texas.
- Verbelen, L., Dadbakhsh, S., Van den Eynde, M., Kruth, J.-P., Goderis, B., Van Puyvelde, P., 2016. Characterization of polyamide powders for determination of laser sintering processability. *European Polymer Journal* 75, 163-174.
- Wang, C.Y., Dong, Q., Shen, X.X., 2011. Research on warpage of polystyrene in selective laser sintering. *Applied Mechanics and Materials* 43, 578-582.
- Wudy, K., Drummer, D., Drexler, M., 2014. Characterization of polymer materials and powders for selective laser melting. *AIP Conference Proceedings* 1593, 702-707.
- Zhu, W., Yan, C., Shi, Y., Wen, S., Liu, J., Shi, Y., 2015. Investigation into mechanical and microstructural properties of polypropylene manufactured by selective laser sintering in comparison with injection molding counterparts. *Materials & Design* 82, 37-45.
- Ziegelmeier, S., Christou, P., Wöllecke, F., Tuck, C., Goodridge, R., Hague, R., Krampe, E., Wintermantel, E., 2015. An experimental study into the effects of bulk and flow behaviour of laser sintering polymer powders on resulting part properties. *Journal of Materials Processing Technology* 215, 239-250.
- Ziegelmeier, S., Wöllecke, F., Tuck, C., Goodridge, R., Hague, R., 2013. Characterizing the bulk & flow behaviour of LS polymer powders. *Proceedings SFF Symposium*, Austin (TX), USA.
- Ziegelmeier, S., Wöllecke, F., Tuck, C.J., Goodridge, R.D., Hague, R.J.M., 2014. Aging behavior of thermoplastic elastomers in the laser sintering process. *Journal of Materials Research* 29, 1841-1851.